Supporting Information

Ultralong near-infrared persistent luminescence in a Cr^{3+}-doped gallogermanate for multifunctional applications

Fangyi Zhao,[a] Yuhe Shao,[b] Qinan Mao,[a] Yiwen Zhu,[a] Heyi Yang,[a] Yang Ding,[a] Quanlin Liu[b]* and Jiasong Zhong[a]*

[a]Center of Advanced Optoelectronic Materials, College of Materials and Environmental Engineering, Hangzhou Dianzi University, Hangzhou 310018, China. E-mail: jiasongzhong@hdu.edu.cn.
[b]The Beijing Municipal Key Laboratory of New Energy Materials and Technologies, School of Materials Science and Engineering, University of Science and Technology Beijing, Beijing 100083, China. E-mail: qlliu@ustb.edu.cn.

Table S1. Main parameters of processing and refinement of MGGO:0.15Cr^{3+} phosphor

Phosphor	MGGO:0.15Cr^{3+}
Space Group	*P*-1
Symmetry	Triclinic
a (Å)	8.8470(2)
b (Å)	9.8184(2)
c (Å)	10.2831(1)
α (°)	63.803(2)
β (°)	84.754(2)
γ (°)	65.363(1)
V (Å^3)	723.81(3)
R_p (%)	7.06
R_{wp} (%)	9.36
R_{exp} (%)	5.35
χ^2	3.07

Table S2. Refined atomic parameters of MGGO:0.15Cr^{3+} phosphor

Atom	Wyck.	Occ.	*x*	*y*	*z*
Mg1	2i	0.206	0.8328	0.8516	0.4607
Ga1	2i	0.794	0.8328	0.8516	0.4607
Mg2	2i	0.188	0.1461	0.1612	0.0501
Ga2	2i	0.812	0.1461	0.1612	0.0501
Mg3	2i	0.601	0.9591	0.9392	0.6501
Ga3	2i	0.399	0.9591	0.9392	0.6501
Mg4	2i	0.923	0.9479	0.9313	0.1600
Ga4	2i	0.077	0.9479	0.9313	0.1600
Mg5	2i	1	0.6397	0.6381	0.5687
Mg6	2i	1	0.6448	0.6164	0.0617
Mg7	2i	0.1	0.7392	0.7483	0.2554
Ga5	2i	0.9	0.7392	0.7483	0.2554
Mg8	1d	0.466	0.5000	0.0000	0.0000
Ga6	1d	0.534	0.5000	0.0000	0.0000
Mg9	1g	0.37	0.0000	0.5000	0.5000
Ga7	1g	0.63	0.0000	0.5000	0.5000
Ga8	2i	0.54	0.7528	0.3570	0.4262
Ge1	2i	0.46	0.7528	0.3570	0.4262
Ga9	2i	0.4	0.7496	0.3529	0.9220
Ge2	2i	0.6	0.7496	0.3529	0.9220
Ga10	2i	0.46	0.6449	0.2510	0.2156
Ge3	2i	0.54	0.6449	0.2510	0.2156
Ga11	2i	0.55	0.6384	0.2481	0.7157
Ge4	2i	0.45	0.6384	0.2481	0.7157
Ga12	2i	0.82	0.9483	0.5670	0.8058
Ge5	2i	0.18	0.9483	0.5670	0.8058
Ga13	2i	0.78	0.5708	0.9400	0.6910
Ge6	2i	0.22	0.5708	0.9400	0.6910
O1	2i	1	0.6186	0.8780	0.3423
O2	2i	1	0.6248	0.8631	0.8746

O3	2i	1	0.8327	0.0614	0.2854
O4	2i	1	0.8367	0.0540	0.7772
O5	2i	1	0.7206	0.9553	0.5574
O6	2i	1	0.7497	0.9380	0.0830
O7	2i	1	-0.0835	0.1736	0.4528
O8	2i	1	-0.0589	0.1831	-0.0113
O9	2i	1	0.8690	0.6226	0.6177
O10	2i	1	0.8503	0.6318	0.1135
O11	2i	1	0.6727	0.3908	0.7537
O12	2i	1	0.6740	0.4278	0.2242
O13	2i	1	-0.0468	0.7310	0.8259
O14	2i	1	-0.0725	0.7357	0.3170
O15	2i	1	0.7851	0.4931	-0.0988
O16	2i	1	0.7593	0.5258	0.4475
O17	2i	1	0.5893	0.3238	0.5368
O18	2i	1	0.5957	0.3115	0.0203
O19	2i	1	0.4782	0.2129	0.3201
O20	2i	1	0.5440	0.7904	0.1642

Table S3. Refined octahedral bond lengths ($d_{1,2}$), average octahedral bond lengths (d_{ave}), octahedral volumes (V), bond length distortion index (D), and bond angle variance (σ^2) of MGGO:0.15Cr^{3+} phosphor

Atom 1	Atom 2	Count	$d_{1,2}$ (Å)	d_{ave} (Å)	V (Å^3)	D	σ^2 (deg.^{2})
Ga1|Mg1	O5	1x	1.6972	2.0779	11.5741	0.07545	56.9177
	O9	1x	2.0136				
	O3	1x	2.0527				
	O14	1x	2.1548				
	O1	1x	2.2078				
	O7	1x	2.3414				
Ga2|Mg2	O8	1x	1.8703	1.9851	10.2993	0.03127	28.1303
	O13	1x	1.9318				
	O6	1x	1.9670				
	O10	1x	1.9961				
	O4	1x	2.0273				
	O2	1x	2.1181				
Ga3|Mg3	O7	1x	1.8338	2.0775	11.7715	0.05756	28.3441
	O3	1x	2.0107				
	O4	1x	2.0430				
	O13	1x	2.0638				
	O7	1x	2.2019				
	O5	1x	2.3118				
Ga4|Mg4	O6	1x	1.9537	2.1123	11.9537	0.04980	111.9103
	O14	1x	1.9558				
	O3	1x	2.1119				
	O4	1x	2.1466				
	O8	1x	2.2106				
	O8	1x	2.2954				
Ga5|Mg7	O14	1x	1.7729	1.9482	9.6585	0.07285	36.3881
	O1	1x	1.8042				
	O20	1x	1.8416				
	O6	1x	1.9542				
	O16	1x	2.1529				
	O10	1x	2.1631				

Ga6|Mg8	O20	2x	1.9030				
	O2	2x	2.1732	2.0848	11.8096	0.05814	41.0373
	O6	2x	2.1783				
Ga7|Mg9	O9	2x	2.0309				
	O14	2x	2.1089	2.0895	11.9655	0.01870	38.8997
	O16	2x	2.1288				
Mg5	O16	1x	1.9713				
	O9	1x	2.0633				
	O19	1x	2.1267	2.1709	13.3808	0.05395	35.4204
	O17	1x	2.1979				
	O11	1x	2.2429				
	O1	1x	2.4233				
Mg6	O12	1x	1.7992				
	O10	1x	2.0226				
	O18	1x	2.0698	2.1370	12.5473	0.08103	74.4877
	O20	1x	2.2303				
	O2	1x	2.2780				
	O15	1x	2.4223				

Table S4. Photoelectric performance of several NIR pc-LED devices fabricated with blue LED chips and Cr^{3+}-doped phosphors.

Phosphors	NIR output power/photoelectric efficiency of pc-LED	Refs
MGGO:Cr^{3+}	6.72 mW/6.55% at 20 mA, 33.34 mW/6.25% at 100 mA, 97.13 mW/5.01% at 350 mA, 107.57 mW/4.82% at 400 mA, 121.60 mW/4.30% at 500 mA	This work
$Ca_2LuZr_2Al_3O_{12}$:Cr^{3+}	2.448 mW/4.1% at 20 mA	[1]
$Y_3MgAl_3SiO_{12}$:Cr^{3+}	8.8 mW/3.16% at 100 mA	[2]
$Na_3Al_2Li_3F_{12}$:Cr^{3+}	36.84 mW/3.5% at 350 mA	[3]
K_3AlF_6:Cr^{3+}	7 mW/~0.67% at 350 mA	[4]
K_3GaF_6:Cr^{3+}	8.4 mW/~0.8% at 350 mA	[4]
$LiInP_2O_7$:Cr^{3+}	6.24 mW/2.2% at 100 mA	[5]
$NaInP_2O_7$:Cr^{3+}	9.08 mW/2.98% at 100 mA	[6]
$NaScSi_2O_6$:Cr^{3+}	26 mW/8.6% at 100 mA	[7]
$ScBO_3$:Cr^{3+}	26 mW/7% at 120 mA	[8]
$Y_{0.57}La_{0.72}Sc_{2.71}(BO_3)_4$:$Cr^{3+}$	10.69 mW/~3.71% at 100 mA, 17.61 mW/~1.81% at 300 mA	[9]
$BaSnSi_3O_9$:Cr^{3+}	12.19 mW/1.37% at 320 mA	[10]
$BaZrGe_3O_9$:Cr^{3+}	6.45 mW/~0.6% at 320 mA	[11]
Ga_4GeO_8:Cr^{3+}	55.94 mW/~3.75% at 400 mA	[12]

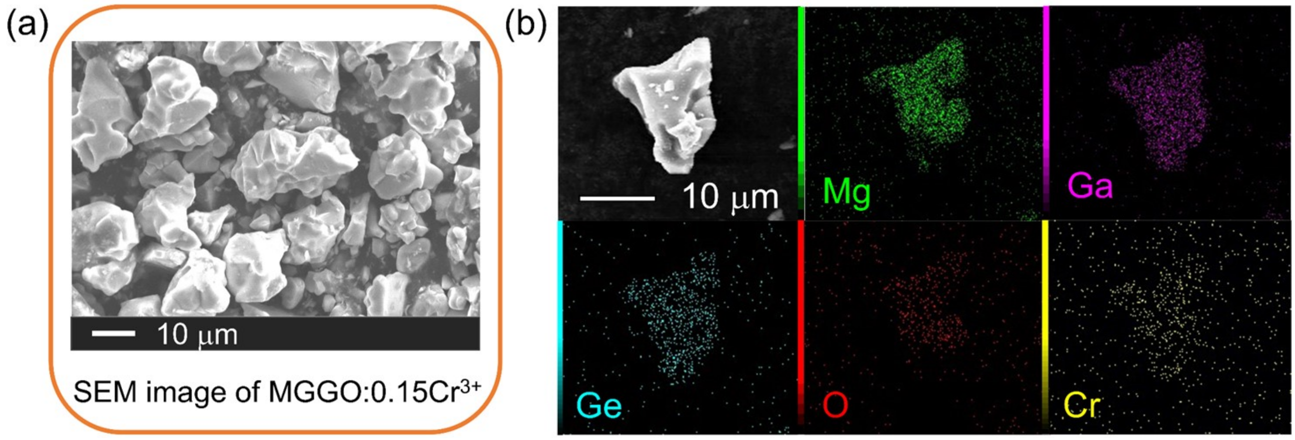

Fig. S1 (a) SEM and (b) element mapping images of MGGO:$0.15Cr^{3+}$.

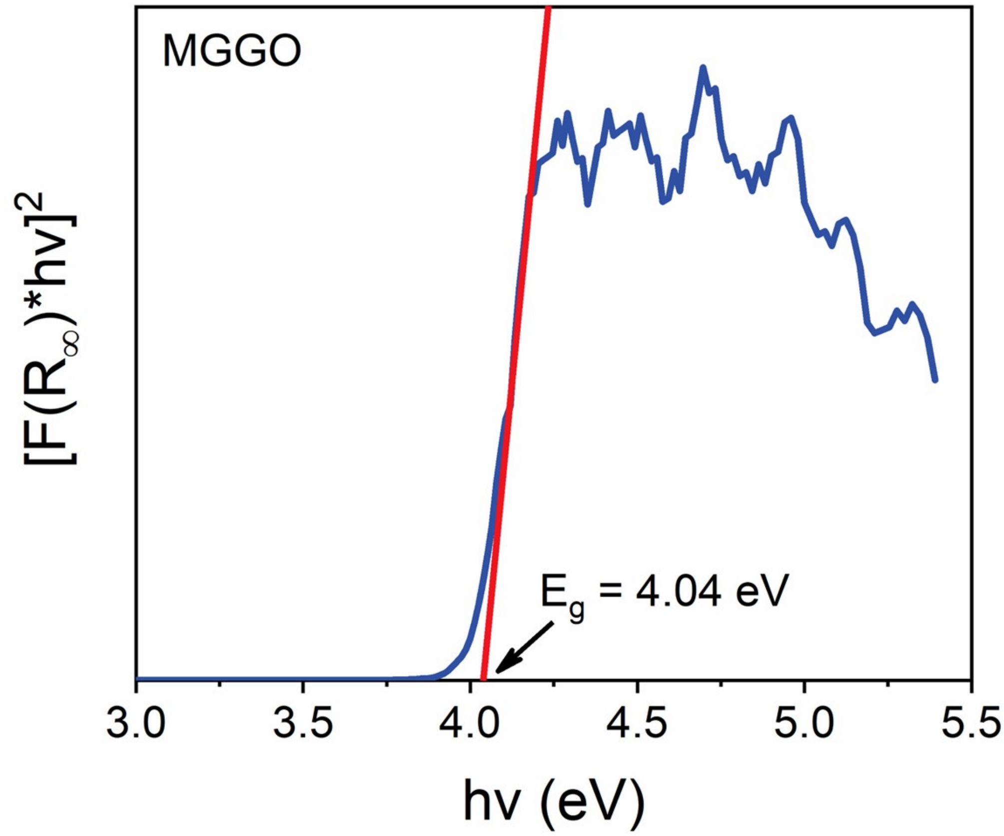

Fig. S2 DR spectrum of MGGO host with $[F(R_\infty)*hv]^2$ as a function of photon energy *hv*.

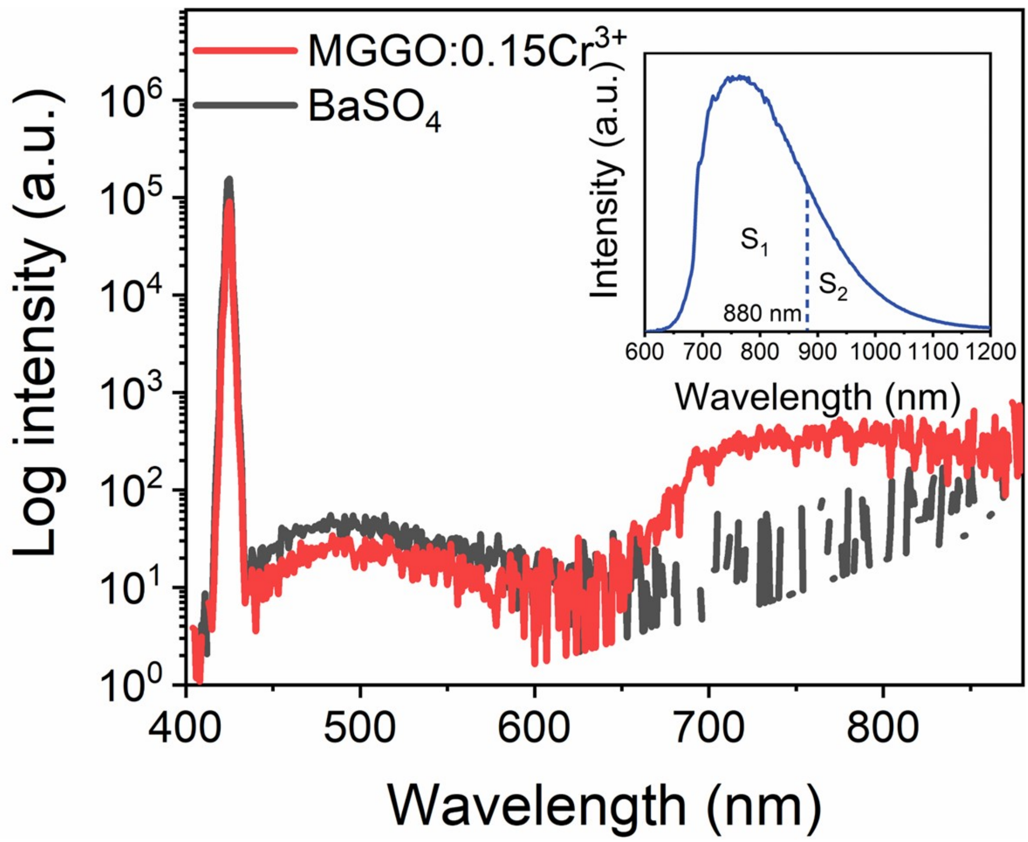

Fig. S3 Spectra of MGGO:0.15Cr^{3+} and $BaSO_4$ to determine the IQE/EQE values, and the inset shows the measured part S1 (600-880 nm) and the missing part S2 (880-1200 nm) of MGGO:0.15Cr^{3+} during the IQE/EQE measurement.

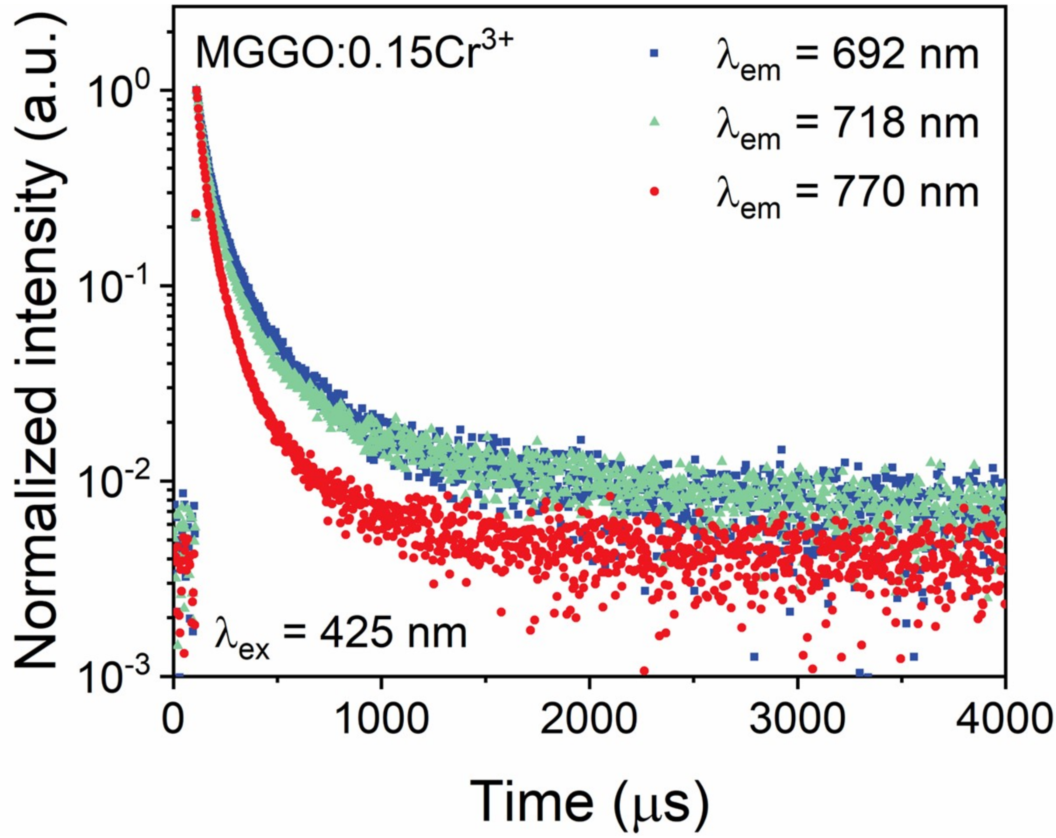

Fig. S4 Luminescence decay curves of MGGO:0.15Cr^{3+} excited by 425 nm and monitoring at 692, 718 and 770 nm, respectively.

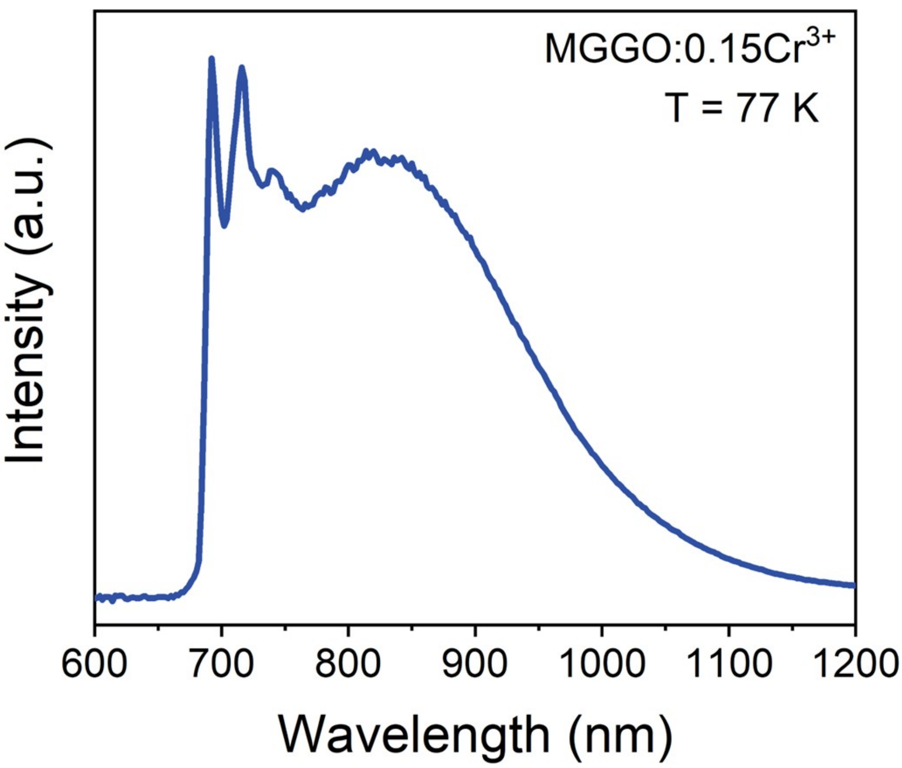

Fig. S5 PL spectrum of MGGO:0.15Cr^{3+} measured at 77 K.

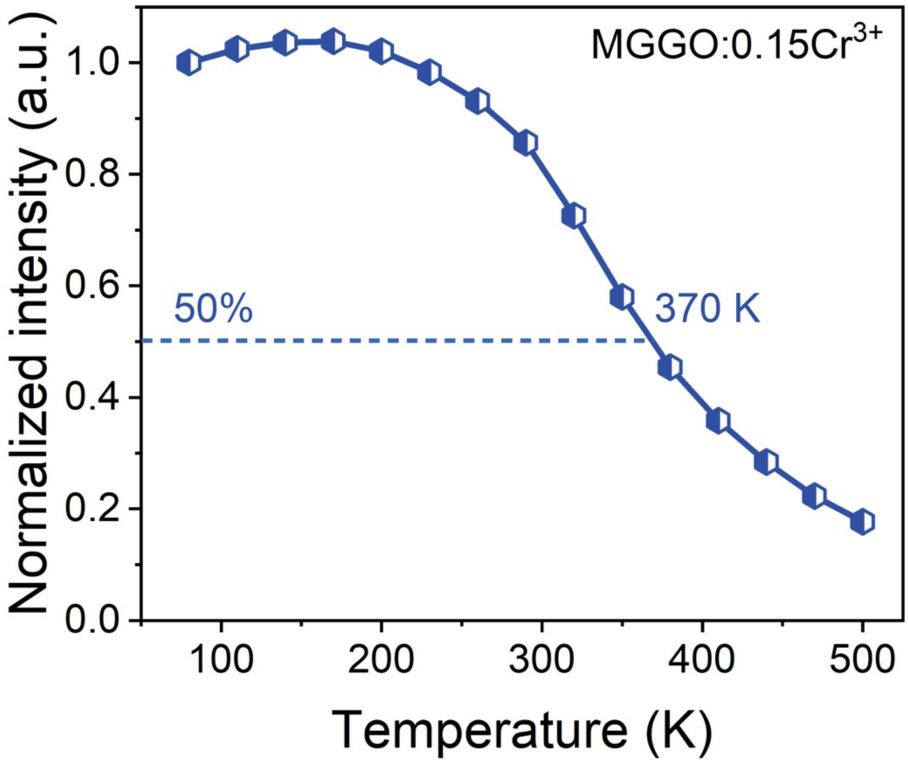

Fig. S6 Relationship between integrated emission intensity and temperature of MGGO:0.15Cr^{3+}.

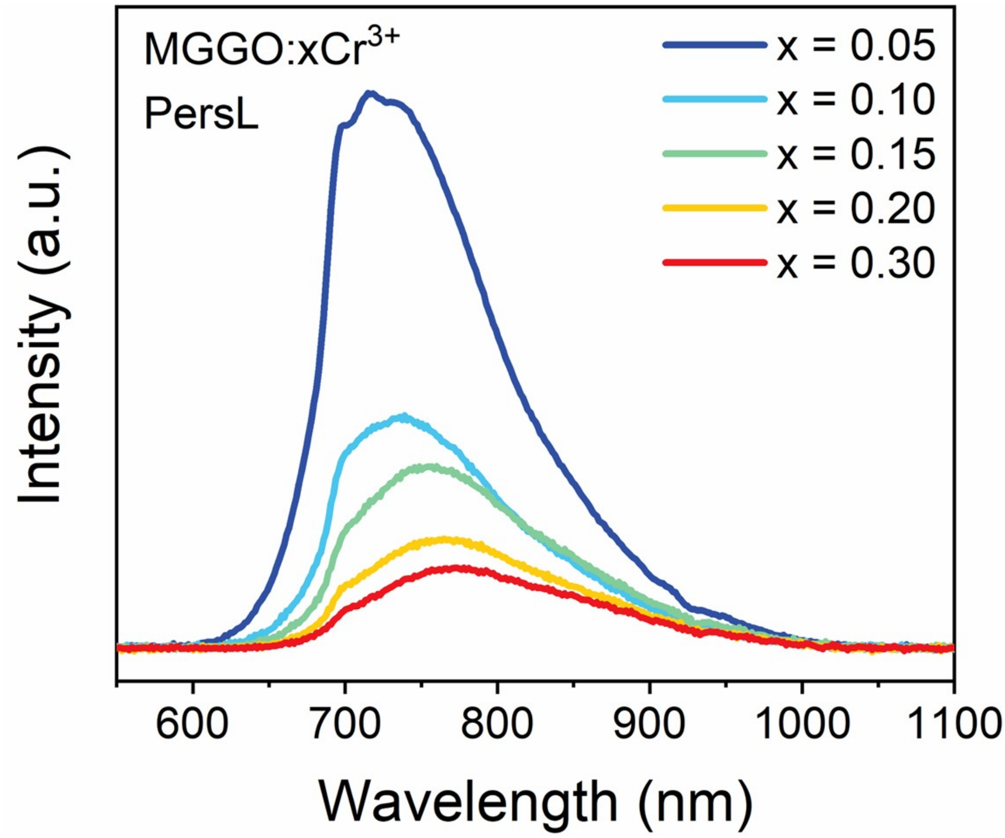

Fig. S7 PersL spectra of MGGO:xCr^{3+} ($0.05 \leq x \leq 0.30$).

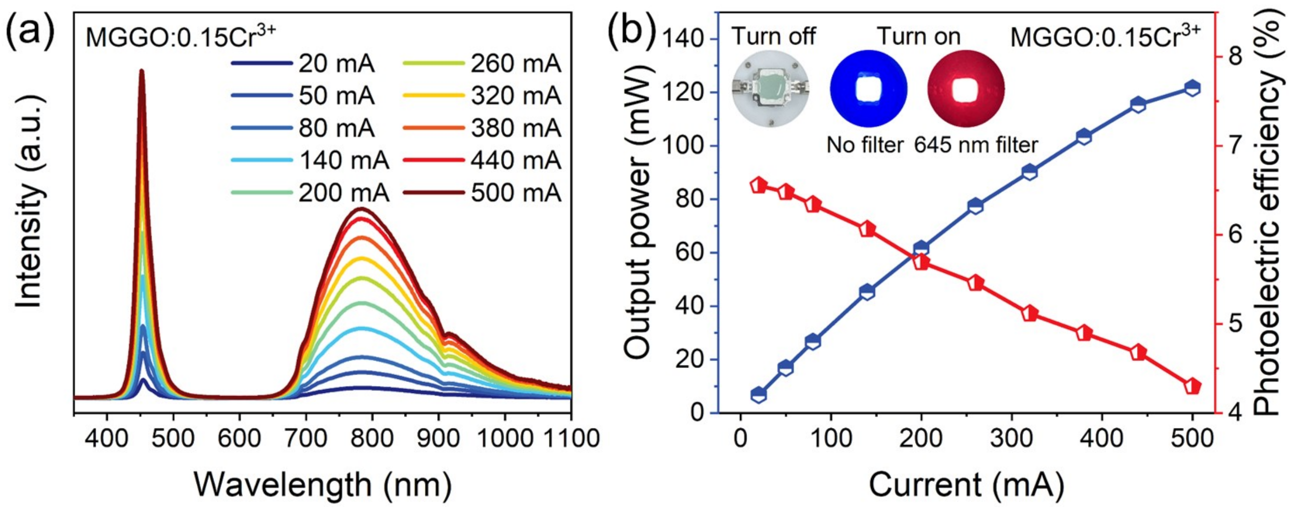

Fig. S8 (a) EL spectra of the NIR pc-LED fabricated by coating MGGO:0.15Cr^{3+} phosphor on a 450 nm blue LED chip at different driving currents (20-500 mA). (b) Output power and photoelectric efficiency as a function of the driving current of the NIR pc-LED, and the inset shows the photographs of this pc-LED with light on and off.

Fig. S9 Photographs of moon, star and arrow films made of MGGO:0.05Cr^{3+} and PDMS.

Calculation method of the optical band gap of MGGO host:

The optical band gap value of the MGGO host can be calculated based on the Kubelka-Munk function and Tauc relation as follows,[13–15]

$$\left[hv * F\left(R_\infty\right)\right]^n = A\left(hv - E_g\right) \tag{S1}$$

$$F\left(R_\infty\right) = \frac{\left(1 - R_\infty\right)^2}{2R_\infty} \tag{S2}$$

where $F(R_\infty)$ represents the Kubelka-Munk function, R_∞ is the reflectance of a layer that completely hides the substrate, h is the Planck's constant, v is the frequency of vibration, hv is the photon energy, A is a proportional constant and E_g is the value of optical band gap.

Calculation method of the IQE/EQE values:

Due to limitations of the instrument, only the IQE/EQE values in the emission wavelength range of 600-880 nm can be measured. The emission regions in 600-880 and 880-1200 nm are denoted as S1 and S2, respectively. The area of S1 occupies 76.28% of the entire emission range of 600-1200 nm, and the IQE/EQE values of S1 are measured to be 23.05%/9.45%. Therefore, the IQE/EQE values of MGGO:0.15Cr^{3+} in the wavelength range of 600-1200 nm are calculated to be 30.22%/12.39%.

Calculation method of the crystal field strength *Dq*/*B*:

The values of octahedral crystal field parameter *Dq*, Racah parameter *B* and crystal field strength *Dq*/*B* can be calculated based on the following Equations,[16,17]

$$10Dq = E\left({}^4T_2\right) = E({}^4A_2 \rightarrow {}^4T_2) - \Delta S / 2 \tag{S3}$$

$$Dq / B = \frac{15(\Delta E / Dq - 8)}{(\Delta E / Dq)^2 - 10(\Delta E / Dq)} \tag{S4}$$

$$\Delta E = E({}^4T_1) - E({}^4T_2) \tag{S5}$$

where $E(^4T_1)$ and $E(^4T_2)$ can be determined from the excitation spectral peaks originating from $^4A_2(^4F) \rightarrow {}^4T_1(^4F)$ and $^4A_2(^4F) \rightarrow {}^4T_2(^4F)$ transitions. Δ*R* is the Stokes shift.

Calculation method of the trap depth:

The trap depth can be calculated based on the following Equation,[18]

$$E = \left(-0.94 \ln \beta + 30.09\right) k T_{\mathrm{m}} \qquad \text{(S6)}$$

where E is the trap depth (eV), β is the heating rate (K/s), k is the Boltzmann's constant with a value of 8.617×10^{-5} eV/K and T_{m} is the temperature (K) of TL glow curve peak.

References

1 L. L. Zhang, S. Zhang, Z. D. Hao, X. Zhang, G. H. Pan, Y. S. Luo, H. J. Wu and J. H. Zhang, A high efficiency broad-band near-infrared $Ca_2LuZr_2Al_3O_{12}:Cr^{3+}$ garnet phosphor for blue LED chips, *J. Mater. Chem. C*, 2018, **6**, 4967–4976.

2 L. P. Jiang, X. Jiang, J. H. Xie, T. Zheng, G. C. Lv and Y. J. Su, Structural induced tunable NIR luminescence of $(Y,Lu)_3(Mg,Al)_2(Al,Si)_3O_{12}:Cr^{3+}$ phosphors, *J. Lumin.*, 2022, **247**, 118911.

3 W. D. Nie, Y. Li, J. X. Zuo, Y. K. Kong, W. F. Zou, G. Chen, J. Q. Peng, F. Du, L. Han and X. Y. Ye, Cr^{3+}-activated $Na_3X_2Li_3F_{12}$ (X = Al, Ga, or In) garnet phosphors with broadband NIR emission and high luminescence efficiency for potential biomedical application, *J. Mater. Chem. C*, 2021, **9**, 15230–15241.

4 C. Lee, Z. Bao, M.-H. Fang, T. Lesniewski, S. Mahlik, M. Grinberg, G. Leniec, S. M. Kaczmarek, M. G. Brik, Y.-T. Tsai, T.-L. Tsai and R.-S. Liu, Chromium (III)-doped fluoride phosphors with broadband infrared emission for light-emitting diodes, *Inorg. Chem.*, 2020, **59**, 376–385.

5 H. S. Zhang, J. Y. Zhong, X. L. Zhang, H. X. Yang, Z. F. Mu and W. R. Zhao, Achieving an ultra-broadband infrared emission through efficient energy transfer in $LiInP_2O_7:Cr^{3+},Yb^{3+}$ phosphor, *J. Alloys Compd.*, 2022, **894**, 162386.

6 L. W. Zeng, J. Y. Zhong, C. J. Li, Z. Q. Zhuang, L. Chen and W. R. Zhao, Broadband near-infrared emission in the $NaInP_2O_7:Cr^{3+}$ phosphor for light-emitting-diode applications, *J. Lumin.*, 2022, **247**, 118909.

7 Q. Y. Shao, H. Ding, L. Q. Yao, J. F. Xu, C. Liang, Z. H. Li, Y. Dong and J. Q. Jiang, Broadband near-infrared light source derived from Cr^{3+}-doped phosphors and a blue LED chip, *Opt. Lett.*, 2018, **43**, 5251–5254.

8 Q. Y. Shao, H. Ding, L. Q. Yao, J. F. Xu, C. Liang and J. Q. Jiang, Photoluminescence properties of a $ScBO_3:Cr^{3+}$ phosphor and its applications for broadband near-infrared LEDs, *RSC Adv.*, 2018, **8**, 12035–12042.

9 H. Y. Wu, L. H. Jiang, K. Li, C. Y. Li and H. J. Zhang, Design of broadband near-infrared $Y_{0.57}La_{0.72}Sc_{2.71}(BO_3)_4:Cr^{3+}$ phosphors based on one-site occupation and their application in NIR light-emitting diodes, *J. Mater. Chem. C*, 2021, **9**, 11761–11771.

10 Y. Zhang, Y. J. Liang, S. H. Miao, D. X. Chen, S. Yan and J. W. Liu, Broadband near-infrared $BaMSi_3O_9:Cr^{3+}$ (M = Zr, Sn, Hf) phosphors for light-emitting diode applications, *Inorg. Chem. Front.*, 2021, **8**, 5186–5194.

11 D. J. Hou, H. H. Lin, Y. Zhang, J. Y. Li, H. L. Li, J. H. Dong, Z. X. Lin and R. Huang, A broadband near-infrared phosphor $BaZrGe_3O_9:Cr^{3+}$: luminescence and application for light-emitting diodes, *Inorg. Chem. Front.*, 2021, **8**, 2333–2340.

12 L. Q. Yao, Q. Y. Shao, M. L. Shi, T. Q. Shang, Y. Dong, C. Liang, J. H. He and J. Q. Jiang, Efficient ultra-broadband $Ga_4GeO_8:Cr^{3+}$ phosphors with tunable peak wavelengths from 835 to 980 nm for NIR pc-LED application, *Adv. Opt. Mater.*, 2022, **10**, 2102229.

13 J. Tauc, R. Grigorovici and A. Vancu, Optical properties and electronic structure of amorphous germanium, *Phys. Status Solidi B*, 1966, **15**, 627–637.

14 E. Davis and N. F. Mott, Conduction in non-crystalline systems V. Conductivity, optical absorption and photoconductivity in amorphous semiconductors, *Philos. Mag.*, 1970, **22**, 0903–0922.

15 N. Yamashita, Luminescence centers of Ca(S:Se) phosphors activated with impurity ions having s^2 configuration. I. Ca(S:Se):Sb^{3+} phosphors, *J. Phys. Soc. Jpn.*, 1973, **35**, 1089–1097.

16 B. Henderson and G. F. Imbusch, Optical Spectroscopy of Inorganic Solids, Oxford University Press, 1989.

17 M. Zhao, S. Q. Liu, H. Cai, F. Y. Zhao, Z. Song and Q. L. Liu, Efficient broadband near-infrared phosphor $Sr_2ScSbO_6:Cr^{3+}$ for solar-like lighting, *Sci. China Mater.*, 2022, **65**, 748–756.

18 S. Y. Zhang, F. Y. Zhao, S. Q. Liu, Z. Song and Q. L. Liu, An improved method to evaluate trap depth from thermoluminescence, *J. Rare Earths*, 2024, Doi: 10.1016/j.jre.2024.02.004.